Tunable 105 ns optical delay for 80 Gb/s RZ-DQPSK, 40 Gb/s RZ-DPSK, and 40 Gb/s RZ-OOK signals using wavelength conversion and chromatic dispersion

Louis Christen,[1,*] Omer F. Yilmaz,[1] Scott Nuccio,[1] Xiaoxia Wu,[1] Irfan Fazal,[1] Alan E. Willner,[1] Carsten Langrock,[1] and Martin M. Fejer[2]

[1]*Department of Electrical Engineering–Systems, University of Southern California, 3740 McClintock Avenue EEB 500, Los Angeles, California 90089, USA*
[2]*Edward L. Ginzton Laboratory, Stanford University, Stanford, California 94305, USA*
**Corresponding author: lcchrist@usc.edu*

Received November 17, 2008; revised November 17, 2008; accepted November 17, 2008; posted December 19, 2008 (Doc. ID 94147); published February 13, 2009

We demonstrate a variable, optical-delay element using tunable wavelength conversion in a periodically poled lithium niobate waveguide, dispersion-compensating fiber and intrachannel dispersion compensation. A delay of up to 105 ns is demonstrated using 80 Gb/s return-to-zero differential-quadrature phase-shift keying, 40 Gb/s return-to-zero differential phase-shift keying, and 40 Gb/s return-to-zero on–off keying modulation formats. Bit-error rates $<10^{-9}$ are demonstrated for each waveform at various delay settings.

OCIS codes: 060.2330, 060.4259, 060.2360, 190.2620.

Signal processing is a powerful enabler and performance enhancer for a host of communications functions, and performing processing in the optical domain reduces optical-electronic conversion inefficiencies. One of the most basic elements needed to achieve efficient and high-throughput signal processing is a tunable optical delay line, but this element has historically been difficult to realize [1]. Applications of such a delay may include (a) synchronization for bit interleaving or (de)multiplexing, (b) data-packet synchronization [2], and (c) time-slot interchange [3] or buffering [1].

Various techniques have been used to demonstrate tunable optical delays, including (i) selecting among a discrete set of optical propagation paths, which produces only a finite set of delays [4]; (ii) using slow-light-based photonic resonances, in which delays tend to be <1 ns for Gbit/s signals [1]; and (iii) wavelength conversion coupled with chromatic dispersion [5–7]. This last technique uses tunable wavelength conversion combined with interchannel chromatic dispersion and intrachannel dispersion compensation. Published results for conversion/dispersion include 12.47 ns for a 10 Gbit/s on–off keying (OOK) signal using parametric wavelength conversion [5], 4.2 ns for a 3.5 ps pulse train using self-phase modulation [6], 44 ns for a 10 Gbit/s OOK [7], and 105 ns for differential-phase-shift-keying (DPSK), differential-quadrature-phase-shift-keying (DQPSK), and OOK [8] signals using periodically poled lithium niobate (PPLN) waveguides.

Given the present importance of highly sensitive DPSK and spectrally efficient DQPSK, modulation format transparency may be a desirable feature for an optical-delay element [9]. In this Letter, we demonstrate an optically controlled delay element based on tunable wavelength conversion, dispersion-compensating fiber (DCF), and intrachannel dispersion compensation, enabling a delay of up to 105 ns using 80 Gb/s return-to-zero (RZ)-DQPSK, 40 Gb/s RZ-OOK, and 40 Gb/s RZ-DPSK modulation formats [8].

Shown in Fig. 1 is a conceptual block diagram of this technique. An input signal (λ_o) is wavelength converted in a PPLN waveguide through sum-frequency generation followed by difference-frequency generation. The output wavelength of the PPLN waveguide is tunable through the choice of the dummy signal (λ_{d1}). The converted signal (λ_c) is filtered out before being sent through a fixed length of DCF. The high chromatic dispersion of the DCF results in a wavelength-dependent group delay. Through tuning of the conversion wavelength of the first stage, the relative delay experienced through

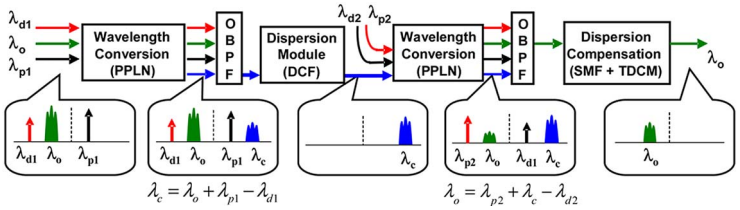

Fig. 1. (Color online) Conceptual diagram of tunable delay using wavelength conversion plus dispersion. λ_o is the input signal; λ_{p1}, λ_{d1}, λ_{p2}, and λ_{d2} are the pump and dummy wavelengths for the first and second PPLN waveguide, respectively; and λ_c is the converted wavelength. OBPF, optical bandpass filter.

0146-9592/09/040542-3/$15.00

the system can be varied. A second wavelength converter is used to convert the delayed signal back to the original wavelength. Following this second conversion, intrachannel dispersion is enabled using a fixed length of standard single-mode fiber (SMF), followed by a tunable dispersion-compensating module (TDCM). As illustrated in Fig. 2, the maximum amount of delay ($\Delta\tau$) through the system is determined by the product of the wavelength-conversion bandwidth ($\Delta\lambda$) and the dispersion (D): $\Delta\tau=\Delta\lambda\times D$, while the delay resolution is limited by the granularity of the wavelength conversion.

An experimental block diagram of the setup is shown in Fig. 3. At the transmitter both 40 Gb/s OOK and DPSK are generated using a Mach–Zehnder modulator (MZM) driven by a 40 Gb/s pseudorandom binary sequence $2^{15}-1$ data stream. To generate 80 Gb/s DQPSK an extra phase modulator (PM) is inserted in series, driven with a delayed version (~500 bits) of the original data. Precoding was not implemented at the transmitter, and programming of the error detector to the expected decoded I and Q patterns was therefore required. Full-rate 40 Gb/s pulse carving is used to 50% RZ pulse carving. Tunable wavelength conversion is achieved using a PPLN waveguide with a quasi-phase-matched (QPM) wavelength of ~1551 nm. Two-pump wavelength conversion is used, based on a cascaded $\chi^{(2)}$ nonlinear process, to produce a converted wavelength at the mirror-image spectral location relative to the QPM wavelength [7]. The input signal (λ_o = 1557.2 nm) serves as the first pump, and the other pump (λ_{p1}=1544.8 nm) is placed equidistant to the QPM wavelength. A dummy signal (λ_{d1}) is then tuned to be equidistant and opposite to the QPM wavelength, relative to the desired conversion location (λ_c).

The converted signal is filtered out using an optical bandpass filter (1.2 nm, 3 dB bandwidth) and sent through 35 km of DCF [–3150 ps/nm of dispersion, insertion loss of –21 dB, and dispersion slope of –0.33 ps/(nm^2 km)]. Following the DCF, the delayed signal is converted back to the original wavelength using a second PPLN waveguide. A 185 km spool of SMF with sign dispersion equal but opposite to that of the DCF is used for compensation of intrachannel dispersion. Open to the dispersion slope of the DCF, there is a residual dispersion of approximately ±200 ps/nm over the tuning range of the delay element. To compensate for this residual dispersion a TDCM is utilized following the SMF. The TDCM had a tuning range of ±400 ps/nm, resolution of 10 ps/nm, a 3 dB bandwidth of 1.6 nm, and a response time of ~1 s. Note that a faster response time may be desirable for some delay applications, and dispersion compensation has been demonstrated with much faster response time [10].

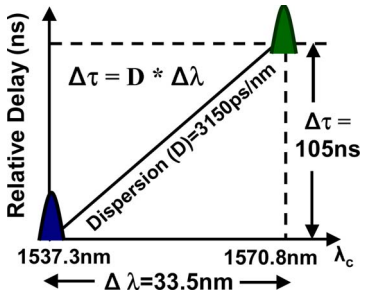

Fig. 2. (Color online) The amount of delay depends on the wavelength conversion range and the total dispersion of the DCF.

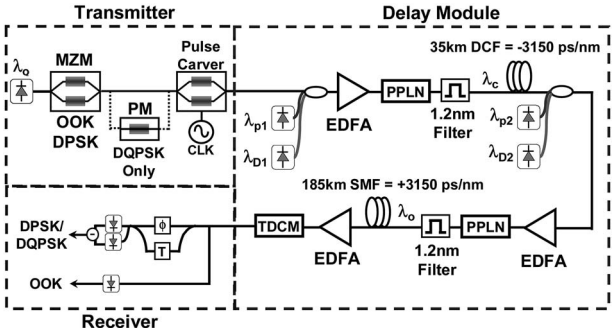

Fig. 3. Experimental setup. Transmitter is capable of generating 80 Gb/s RZ-DQPSK, 40 Gb/s RZ-DPSK, and 40 Gb/s RZ-OOK modulation formats. Phase demodulation at the receiver for DPSK/DQPSK is performed with a single interferometer tuned to the appropriate location (I and Q measured separately).

The output of the TDCM is detected and sent to an error detector to measure the bit-error rate (BER). For OOK, a simple photoreceiver is used. For DPSK and DQPSK, a 25 ps delay-line interferometer (DLI) is used for phase demodulation prior to detection using a balanced photoreceiver. Because we are limited to a single DLI at the receiver, the in-phase (I) and quadrature (Q) channels for DQPSK are detected at different times through tuning of the DLI phase to ±45°, respectively.

Shown in Fig. 4 is the relative delay of the system as a function of the converted wavelength. Identical delay measurements were performed for all formats, including 80 Gb/s RZ-DQPSK, 40 Gb/s RZ-DPSK, and 40 Gb/s RZ-OOK. It should be noted that the converted wavelength cannot be generated at the QPM wavelength, as it would overlap the dummy. The converted wavelength can also not be generated at the pump wavelength or at the signal input wavelength. The QPM and pump wavelength gaps can be avoided through temperature tuning of the PPLN's

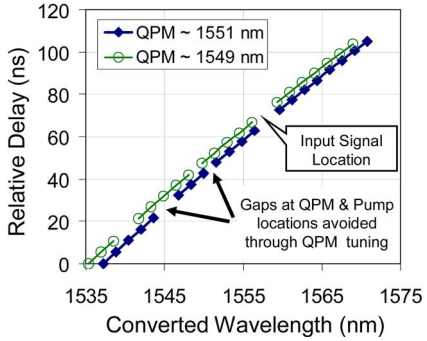

Fig. 4. (Color online) Relative delay versus converted wavelength through the DCF. Tuning gaps due to the pump and QPM location can be avoided through tuning of the PPLN QPM.

QPM wavelength. Figure 4 illustrates the delay response of the system for two different QPM wavelengths, 1549 and 1551 nm. The resulting tuning gaps at the QPM and pump wavelengths do not overlap for these two conditions. Note that the QPM wavelength of the PPLN is tunable over approximately 10 nm for a temperature range of 20°C to 100°C.

A maximum delay value of 105 ns was achieved, which is in agreement with the bandwidth-dispersion product of (33.5 nm)×(3150 ps/nm). This maximum delay was limited by the 33.5 nm amplification bandwidth of the erbium-doped fiber amplifier following the first wavelength conversion. Shown in Fig. 5(a) are sample optical spectra at the output of the first and second wavelength conversion stages. Both PPLN waveguides were fiber pigtailed at both input and output and were temperature controlled to have a QPM location of ~1551 nm. Note that the wavelength conversion bandwidth of the PPLN is approximately 80 nm and the QPM wavelength of the PPLN is tunable over approximately 10 nm for a temperature range of 20°C to 100°C.

To assess the impact of the delay module on data quality, we measured the BER both before and after the delay element for 80 Gb/s RZ-DQPSK [Fig. 5(b)], 40 Gb/s RZ-DPSK, and 40 Gb/s RZ-OOK (Fig. 6) modulation formats. Power penalties from 3 to 7 dB are observed at a BER of 10^{-9}, while little power penalty was observed at higher BERs. Despite BER flaring, no error floor existed and BER $<10^{-9}$ was obtained for all formats at various delay settings. No penalty was observed after the first wavelength conversion, and we believe the system penalty to be due to the cascaded filters and amplifiers in the delay module, along with finite residual dispersion. We note that it is possible to reduce the complexity of the setup by double passing through the same span of DCF for both delay and dispersion compensation. However, this requires phase conjugation in the second conversion stage.

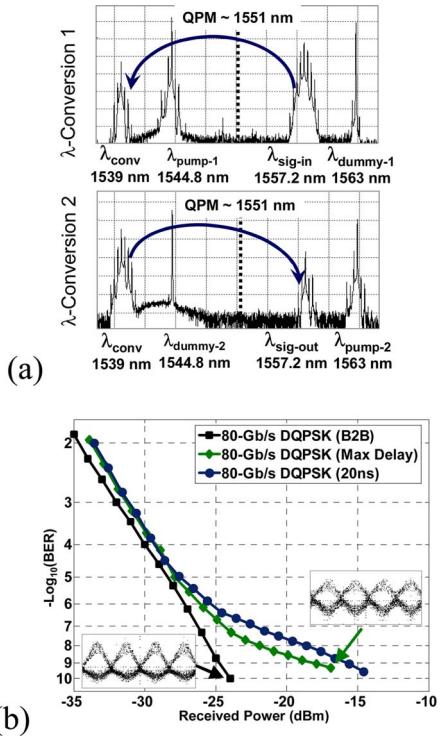

Fig. 5. (Color online) (a) Experimental optical spectra after both wavelength conversion stages. (b) BER performance for 80 Gb/s RZ-DQPSK (average of I and Q tributaries reported).

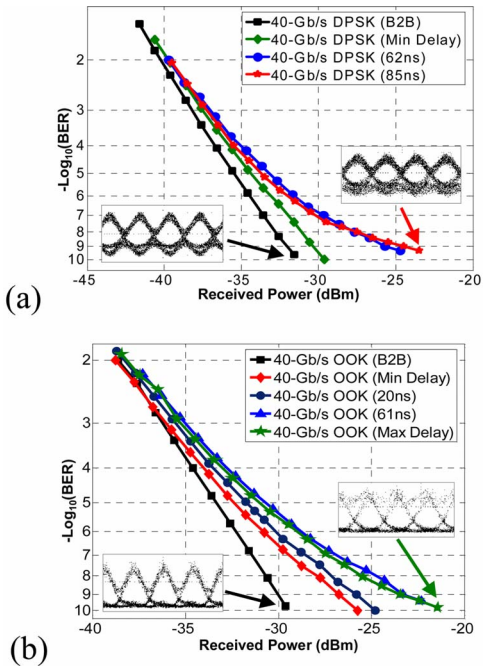

Fig. 6. (Color online) BER performance for (a) 40 Gb/s RZ-DPSK and (b) 40 Gb/s RZ-OOK.

References

1. C. Chang-Hasnain, P. Ku, and R. S. Tucker, J. Lightwave Technol. **23**, 4046 (2005).
2. I. Fazal, O. Yilmaz, S. Nuccio, B. Zhang, A. E. Willner, C. Langrock, and M. M. Fejer, Opt. Express **15**, 10492 (2007).
3. L. Christen, O. F. Yilmaz, S. Nuccio, X. Wu, I. Fazal, and A. E. Willner, in *Proceedings of Conference on Optical Fiber Communications* (IEEE/OSA, 2008), paper OThA4.
4. M. Houmaidi, M. A. Bassiouni, and G. Li, Photonic Network Commun. **13**, 111 (2007).
5. J. Ren, N. Alic, E. Myslivets, R. E. Saperstein, C. J. McKinstrie, R. M. Jopson, A. H. Gnauck, P. A. Andrekson, and S. Radic, *Proceedings of European Conference on Optical Communication* (ECOC, 2006), paper Th4.4.3.
6. Y. Okawachi, J. E. Sharping, C. Xu, and A. L. Gaeta, Opt. Express **14**, 12022 (2006).
7. Y. Wang, C. Yu, L. S. Yan, A. E. Willner, R. Roussev, C. Langrock, M. M. Fejer, J. E. Sharping, and A. L. Gaeta, IEEE Photon. Technol. Lett. **19**, 861 (2007).
8. L. Christen, I. Fazal, O. Yilmaz, X. Wu, S. Nuccio, A. E. Willner, C. Langrock, and M. M. Fejer, in *Proceedings of Conference on Optical Fiber Communications* (IEEE/OSA, 2008), paper OTuD1.
9. B. Zhang, L. Yan, I. Fazal, L. Zhang, A. E. Willner, Z. Zhu, and D. J. Gauthier, Opt. Express **15**, 1878 (2006).
10. S. Namiki, in *Proceedings of Conference on Optical Fiber Communications* (IEEE/OSA, 2008), paper OWP1.